ЖЭТФ/JETP, 2026, том 170, вып. 3 (9), стр. 266–272

MAGNETOCALORIC EFFECT FOR THE ALTERMAGNETIC CANDIDATE MnTe

N. N. Orlova [a], ***V. D. Esin*** [a], ***A. V. Timonina*** [a], ***N. N. Kolesnikov*** [a], ***E. V. Deviatov*** [a,b*]

[a] *Institute of Solid State Physics of the Russian Academy of Sciences*
142432, Chernogolovka, Moscow Region, Russia

[b] *V. L. Ginzburg Research Centre for High-Temperature Superconductivity and Quantum Materials,*
P. N. Lebedev Physical Institute of the Russian Academy of Sciences
119991, Moscow, Russia

Received June 23, 2026,
revised version July 12, 2026
Accepted for publication July 30, 2026

We experimentally investigate magnetocaloric effect for single crystals of altermagnetic candidate MnTe at the transition to the state with spontaneous spin polarization, i. e., well below the Néel temperature of MnTe. The isothermal magnetic entropy change ΔS is calculated from the experimental magnetization curves by using Maxwell relation. We observe well-defined magnetocaloric effect as a narrow ΔS peak around the critical temperature $T_c \approx 81$ K, which reflects the sharp magnetization jump. This behavior is unusual for standard ferromagnetic transitions, so it confirms the predicted spin-orbit-induced spin polarization in the MnTe altermagnetic state and, therefore, confirms MnTe as a prototypical altermagnet candidate.

Keywords: altermagnetism, magnetocaloric effect, magnetic entropy change, spontaneous magnetization

DOI: 10.31857/S0044451026090066

1. INTRODUCTION

Recently, a new class of altermagnetic materials has been proposed [1, 2]. The usual ferro- and antiferromagnetic classes are not characterized by noticeable spin-orbit coupling, i. e., they belong to non-relativistic groups of magnetic symmetry. In contrast, one of the central concepts of the topological materials is the spin-momentum locking [3], which, usually, appears due to spin-orbit coupling [4]. In altermagnets, the concept of spin-momentum locking was extended to the case of weak spin-orbit coupling, e. g., in collinear antiferromagnets. As a result, altermagnets are characterized by alternating spin splitting in the k-space [1, 5], so the up-spin-polarized subband and the down-polarized one are connected by ($\pi/2$, $\pi/3$, etc.) rotation in the reciprocal space [6, 7].

Despite the initial theoretical proposal, spin-orbit coupling still can be important in real altermagnetic materials. For example, observation of the anomalous Hall effect (AHE) [4] is regarded [8, 9] as one of the main experimental demonstrations of altermagnetism for non-ferromagnetic materials [10–12]. However, it is a common agreement, that AHE still requires finite net magnetization [13], which appears due to the finite spin-orbit coupling in altermagnets [14].

MnTe is regarded as a prototypical altermagnet candidate [15], while for years it was known as a collinear antiferromagnet [16–21]. The magnetic moments on Mn have a parallel alignment within the c planes and an antiparallel alignment between the planes, so the two magnetic sublattices are connected by a sixfold screw axis along [0001] in real space. At low temperatures, MnTe shows spontaneous AHE signals at zero magnetic field [10, 11] and spontaneous ferromagnetic-like magnetization [22, 23], which are the main experimental confirmations of altermagnetism in MnTe. Since spontaneous magnetization still requires spin-orbit coupling, it has been investigated in MnTe by temperature-dependent angle-resolved photo-emission spectroscopy (ARPES) and by disordered local moment calculations [24]. It seems to be important, that spin-orbit coupling is well-resolved [24] only below 100 K, which is consistent with appearance of spontaneous

* E-mail: dev@issp.ac.ru

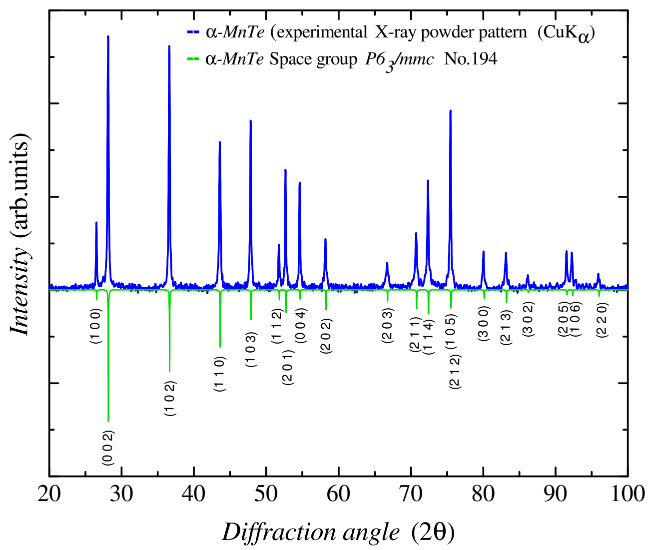

Fig. 1. (Color online) The X-ray powder diffraction pattern (Cu K_α radiation), which is obtained for the crushed MnTe single crystal. The single-phase α-MnTe is confirmed with the space group $P6_3/mmc$ No. 194, so the results below cannot appear from the incorrect stoichiometry or oxides

magnetization [22,23]. At this transition, the easy magnetization axis is $\pi/2$ rotated [23] either by increasing the field above 1 kOe or the temperature above 81 K. The observed behavior cannot be expected for antiferromagnetics, thus, it requires to take into account the formation of the altermagnetic ground state for MnTe single crystals.

Generally speaking, altermagnetism presents a new type of spin ordering, which should be detectable by observation of the magnetocaloric effect (MCE). The latter is known as the entropy change ΔS while the system undergoes the transition between differently spin ordered states [25]. MCE is of special interest due to the possible applications [26, 27], for example, utilizing of antiferromagnetic coupling should increase energy efficiency of a MCE refrigerator. For the fundamental research, irrespective of the entropy change values, observation of MCE should confirm transition between differently spin-orderd states in altermagnetic materials. For example, it is reasonable to study MCE at the transition to the spin-orbit-induced [24] spin-polarized state [10, 11, 22, 23] around 81 K in altermagnetic candidate MnTe.

Here, we experimentally investigate magnetocaloric effect for single crystals of MnTe altermagnet at the transition to the state with spontaneous spin polarization, i. e., well below the Néel temperature of MnTe. We observe well-defined magnetocaloric effect as a narrow ΔS peak around the cricital temperature $T_c \approx 81$ K, which reflects the sharp magnetization jump.

2. SAMPLES AND TECHNIQUE

α-MnTe was synthesized by reaction of elements (99.99% Mn and 99.9999% Te) in evacuated silica ampules slowly heated up to 1050–1070°C. The obtained loads were melted in the graphite crucibles under 10 MPa argon pressure, then homogenized at 1200°C for 1 hour. The crystals grown by gradient freezing method are groups of single crystal domains with volume up to 0.5–1.0 cm^3. The MnTe composition is verified by energy-dispersive X-ray spectroscopy. The powder X-ray diffraction analysis confirms single-phase α-MnTe with the space group $P6_3/mmc$ No. 194, see Fig. 1. As usual, the powder has been obtained by crashing the MnTe single crystal. High quality of our MnTe single crystals is also confirmed by high reproducibility of the results, which are obtained for MnTe flakes of different mass and shape [22, 23].

The measurements are performed by Lake Shore Cryotronics 8604 VSM magnetometer, equipped with nitrogen flow cryostat. We investigate two mechanically cleaved single crystal MnTe flakes of different mass (2.89 mg and 5.73 mg, respectively) to confirm reproducibility of the results. A flake is mounted to the magnetometer sample holder by a low temperature grease, which has been tested to have a negligible magnetic response [28]. Small single crystal flakes are preferable for sensible measurements, while, e. g., for thin films the results may be seriously affected by the geometrical factors and by the admixture of the sub-

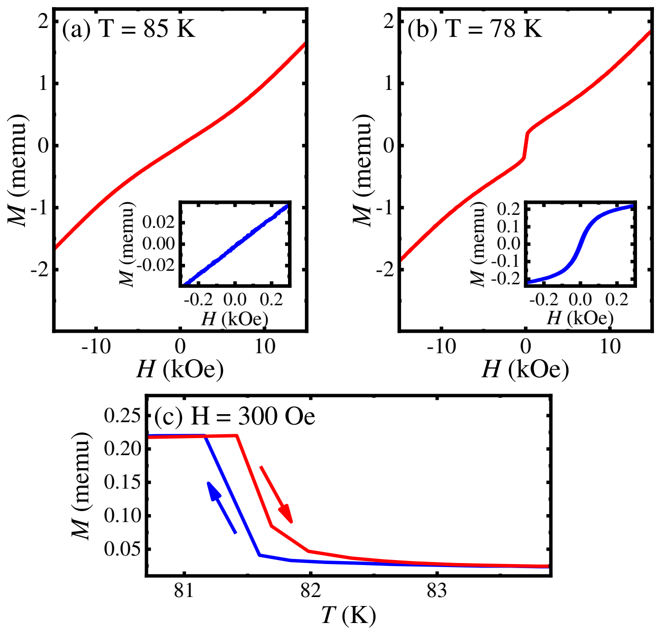

Fig. 2. (Color online) Transition from antiferromagnetic to the ferromagnetic-like magnetization around 81 K for the 5.73 mg MnTe sample, see Refs. [22, 23] for details. *a* — $M(H)$ magnetization curves above the transition, at 85 K temperature. There are nonlinear $M(H)$ branches in high magnetic fields, while $M(H)$ is strictly linear in low fields, as it is depicted in the inset. This $M(H)$ behavior is expected for the antiferromaghetic state. *b* — Nonlinear $M(H)$ branches are shifted vertically at low 78 K temperature, so a pronounced zero-field kink can be seen. The inset shows low-field $M(H)$ ferromagnetic-like hysteresis. *c* — Appearence of spontaneous magnetization below 81 K as a sharp $M(T)$ jump. The red and the blue curves are obtained at 300 Oe magnetic field, for heating and cooling, respectively

strate magnetic response, especially in low magnetic fields [29]. The sample can be rotated in magnetic field, so the hard and easy magnetization directions (i. e., sample orientation) can be obtained [22, 23] from angle-dependent magnetization $M(\alpha)$.

We investigate the magnetocaloric effect as the isothermal magnetic entropy change ΔS which is calculated from the experimental magnetization curves by using Maxwell relation [25, 30, 31]:

$$\Delta S = \mu_0 \int_0^H \left(\frac{\partial M}{\partial T}\right)_H dH. \qquad (1)$$

As a first step, a set of $M(H, T = \text{const})$ isotherms is obtained for the required magnetic field range. Subsequently, the first derivative $\left(\frac{\partial M}{\partial T}\right)_H$ is calculated as a result of subtraction $\left(\frac{\Delta M}{\Delta T}\right)(H, T)$ of every two neighbor curves. As a final step, ΔS is achieved for every temperature point by integration over the magnetic field range [25, 31].

3. EXPERIMENTAL RESULTS

Figure 2 shows appearance [22, 23] of the spontaneous ferromagnetic-like magnetization around 81 K for the 5.73 mg MnTe sample. $M(H)$ magnetization dependences are measured for easy magnetization direction [22, 23] by standard method of the magnetic field gradual sweeping between two opposite field values.

Let us start from higher temperatures, i. e., from the well-known antiferromagnetic state. At 85 K temperature, there are nonlinear $M(H)$ branches in high magnetic fields, see Fig. 2 *a*, while $M(H)$ is strictly linear in low fields, as it is demonstrated in the inset. The linear $M(H)$ is expected for the antiferromaghetic state, while the high-field nonlinear $M(H)$ branches are due to the antiferromagnetic domain configuration change below the Néel vector reorientation field [29, 32].

At low 78 K temperature, there are also nonlinear $M(H)$ branches, but they are shifted vertically, so a pronounced zero-field kink can be seen in Fig. 2 *b*. The low-field $M(H)$ curves are shown in the inset to Fig. 2 *b*, they are obtained with high accuracy for smaller magnetic field step for two sweep directions. The inset con-

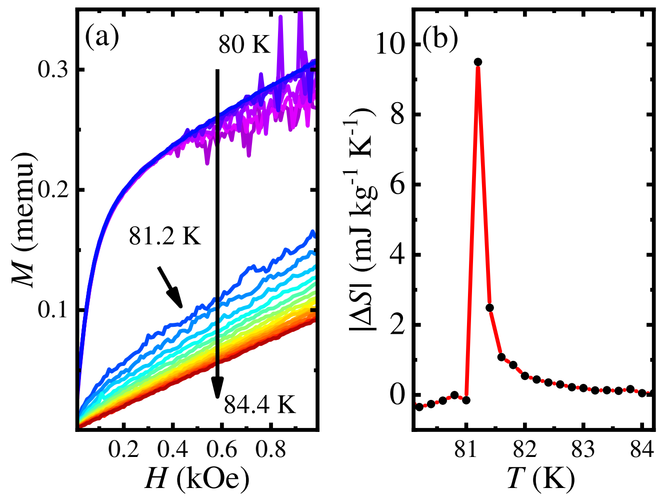

Fig. 3. (Color online) *a* — $M(H,T = \text{const})$ isothermal magnetization curves from 80 to 84.4 K temperatures with 0.2 K step, with sharp $M(T)$ jump at the transition temperature $T_c \approx 81$ K. The initial sample state is obtained after ZFC from room temperature to 78 K. Between the curves, temperature is always stabilized at zero field. *b* — The isothermal magnetic entropy change ΔS with narrow peak at the critical temperature $T_c \approx 81$ K. The obtained $|\Delta S|$ values are much below the usual ones for standard ferromagnetic transitions around the Curie temperature [25]. The data are obtained for the 5.73 mg MnTe sample

firms ferromagnetic-like hysteresis, i. e., spontaneous magnetization, at this temperature [22, 23].

The detailed $M(T)$ temperature dependence is shown in Fig. 2 *c*. The temperature is stabilized with 0.2 K step from 78.4 K to 83.8 K. The red and the blue curves are obtained at 300 Oe magnetic field, for heating and cooling, respectively. It can be seen from the curves, that ferromagnetic-like spontaneous magnetization appears below 80.5–81.5 K as a sharp $M(T)$ jump.

As the main experimental result, we investigate magnetocaloric effect around the transition to the ferromagnetic-like state. $M(H,T = \text{const})$ isothermal magnetization curves are obtained in a temperature range, that covers the transition temperature $T_c \approx 81$ K, see Fig. 3 *a*. Before any set of $M(H,T = \text{const})$ isotherms, it is necessary to set up the stable initial magnetic state of the sample [25]. In our experiment, it is performed by cooling the sample in zero magnetic field (ZFC protocol) from the room temperature to 78 K one, and subsequent sample magnetization along the easy axis by sweeping the field between −15 kOe and +15 kOe values. Afterward, temperature is stabilized with 0.2 K step, $M(H)$ curves are obtained from 80 K to 84.4 K, see Fig. 3 *a*. Between the curves, temperature is always stabilized at zero field.

The isothermal magnetic entropy change ΔS can be calculated by Eq.(1), absolute $|\Delta S|$ values are presented in Fig. 3 *b*. As it should be expected from sharp $M(T)$ jump in Fig. 2 *c* and in Fig. 3 *a*, the obtained $|\Delta S|$ shows narrow peak at the cricital temperature $T_c \approx 81$ K in Fig. 3 *b*. MnTe heat capacity C_p equals [33,34] to 191.3 $\text{J}\cdot\text{kg}^{-1}\cdot\text{K}^{-1}$ for 80 K, so one can estimate [30, 35] $\Delta T = -\frac{T\Delta S}{C_p} \approx 4$ mK at the transition point. Thus, the obtained $|\Delta S|$ and ΔT values are much below the usual ones for standard ferromagnetic transitions around the Curie temperature [25].

The $M(T)$ transition is unusually sharp in our case, which can be directly seen from the original $M(H)$ curves in Fig. 3 *a*. The difference between the temperature points is limited by requirement of temperature stabilization, the quality of stabilization is also confirmed by the original $M(H)$ curves in Fig. 3 *a*. However, there are still several experimental point for the peak region in Fig. 3 *b*. Moreover, the peak's shape well reflects the $M(H)$ curves evolution: the jump in $|\Delta S|$ is sharp between 81K and 81.2 K, while the drop is smoother above 81.2 K in Fig. 3 *b*.

The reported behavior is sample-independent, it can be reproduced for any MnTe single crystal sample. For example, Fig. 4 shows $M(H,T = \text{const})$ isothermal magnetization curves (*a*) and $|\Delta S|$ values (*b*) for the 2.89 mg MnTe sample. For this sample, the temperature range is chosen as 79 K–82.2 K. The transition can be seen as sharp $M(T)$ jump at $T_c \approx 79.5$ K, which well corresponds to the position of

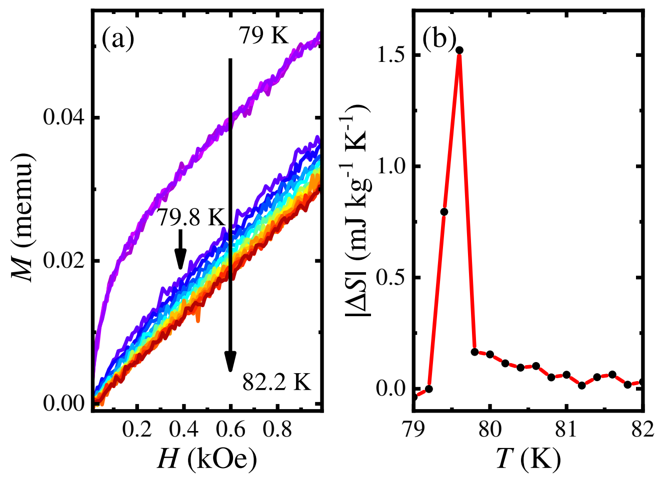

Fig. 4. (Color online) $M(H, T = \text{const})$ isothermal magnetization curves (a) and $|\Delta S|$ values (b) for the 2.89 mg MnTe sample. The transition can be seen as sharp $M(T)$ jump at $T_c \approx 79.5$ K, which well corresponds to the position of the $|\Delta S|$ peak. The peak amplitude is diminished for this 2.89 mg MnTe sample in comparison with the 5.73 mg one in Fig. 3 *b*. The magnetization value does not scale with the sample mass for the ferromagnetic-like state in low fields [22, 23]

the $|\Delta S|$ peak. The peak amplitude is diminished to $|\Delta S(T)| = 1.5\,\text{mJ} \cdot \text{kg}^{-1} \cdot \text{K}^{-1}$ for this 2.89 mg MnTe sample, while it one order of magnitude greater for the 5.73 mg one in Fig. 3 *b*. This difference is due to the fact, that the magnetization $M(H)$ value does not scale with the sample mass for the ferromagnetic-like state in low fields in Figs. 3 *a* and 4 *a*. In contrast, magnetization value is proportional to the sample mass in high fields and/or above the transition temperature T_c (see Refs. [22, 23] for these data).

4. DISCUSSION

As a result, we observe well-defined magnetocaloric effect for MnTe altermagnet candidate as a sharp $|\Delta S|$ peak around 81 K, the effect is well reproducible for different samples with low variation of the critical temperature T_c K.

First of all, the critical temperature $T_c \approx 81$ K is well below the Néel temperature of MnTe, which exceeds the room value [16–21]. Thus, the alignment of magnetic moments on Mn is stable in this temperature range and, therefore, can not be responsible for the observed $|\Delta S|$ peak around 81 K.

Secondly, both sharp $M(T)$ jump and relatively low $|\Delta S|$ peak values are unusual for standard ferromagnetic-paramagnetic transitions, i. e., around the Curie temperature, see Ref. [25] as an example. Thus, the effect could not be connected with any imperfections (magnetic impurities), if they occurred in our MnTe samples. The sample quality is independently confirmed by energy-dispersive X-ray spectroscopy and powder X-ray diffraction analysis [22, 23].

On the other hand, MnTe belongs to a new class of altermagnetic materials [15]. For MnTe it is accepted, that the principle origin of nonzero net magnetic moment [10, 11, 22, 23], and, therefore, of weak remanence magnetization [14, 36] is the spin-orbit coupling [13] in the valence orbitals [37]. It seems to be important, that spin-orbit coupling is well-resolved only below 100 K in Ref. [24], which is consistent with appearance of narrow $|\Delta S|$ peak in Figs. 3 and 4.

Thus, narrow $|\Delta S|$ peak at the critical temperature T_c confirms the transition in the spin ordering from the spin-orbit-induced spin polarization in the MnTe altermagnetic state, and, therefore, confirms MnTe as a prototypical altermagnet candidate [15].

For possible applications of magnetocaloric effect in altermagnets, small amplitude of ΔS and, therefore, of ΔT, can only allow to consider MnTe as a model system, which should stimulate further material search. However, observation of magnetocaloric effect in MnTe opens a new way to transfer from ferromagnetically ordered systems to the altermagnetic ones with higher reversibility and smaller energy costs, which is confirmed by small width of the $|\Delta S|$ peak at the critical temperature T_c in comparison with standard ferromagnetic-paramagnetic transitions.

5. CONCLUSION

As a conclusion, we experimentally investigate magnetocaloric effect for single crystals of MnTe altermagnet at the transition to the state with spontaneous spin polarization, i. e., well below the Néel temperature of MnTe. The isothermal magnetic entropy change ΔS is calculated from the experimental magnetization curves by using Maxwell relation. We observe well-defined magnetocaloric effect as a narrow ΔS peak around the cricital temperature $T_c \approx 81$ K, which is reflects the sharp magnetization jump. This behavior is unusual for standard ferromagnetic transitions, so it confirms the predicted spin-orbit-induced spin polarization in the MnTe altermagnetic state. Despite it is believed, that utilizing of altermagnet should increase the energy efficiency of a refrigerator, MnTe is characterized by small amplitude of the magnetocaloric effect. Thus, MnTe can can only be considered as a model system for magnetocaloric applications, which can stimulate further material search.

Acknowledgements. We wish to thank S. S. Khasanov for X-ray sample characterization and V. Zyuzin for valuable discussions.

Funding. We gratefully acknowledge financial support by the Russian Science Foundation, project RSF-26-12-00001, https://rscf.ru/project/26-12-00001/

Conflicts of interest. The authors declare that they have no conflicts of interests.

Author's contributions. The contributions of the authors are equivalent.

REFERENCES

1. L. Šmejkal, J. Sinova, and T. Jungwirth, *Beyond Conventional Ferromagnetism and Antiferromagnetism: a Phase with Nonrelativistic Spin and Crystal Rotation Symmetry*, Phys. Rev. X **12**, 031042 (2022).

2. I. Mazin, *Editorial: Altermagnetism—a New Punch Line of Fundamental Magnetism*, Phys. Rev. X **12**, 040002 (2022); https://doi.org/10.1103/PhysRevX.12.040002.

3. H.-Y. Ma, M. Hu, N. Li et al., *Multifunctional Antiferromagnetic Materials with Giant Piezomagnetism and Noncollinear Spin Current*, Nat. Commun. **12**, 2846 (2021).

4. N. P. Armitage, E. J. Mele, and A. Vishwanath, *Weyl and Dirac Semimetals in Three-Dimensional Solids*, Rev. Mod. Phys. **90**, 015001 (2018).

5. J. A. Ouassou, A. Brataas, and J. Linder, *DC Josephson Effect in Altermagnets*, Phys. Rev. Lett. **131**, 076003 (2023); https://doi.org/10.1103/PhysRevLett.131.076003.

6. I. I. Mazin, *Notes on Altermagnetism and Superconductivity*, AAPPS Bull. **35**, 18 (2025); https://doi.org/10.1007/s43673-025-00158-6; arXiv:2203.05000.

7. S. Das, D. Suri, and A. Soori, *Transport Across Junctions of Altermagnets with Normal Metals and Ferromagnets*, J. Phys.: Condens. Matter **35**, 435302 (2023); https://doi.org/10.1088/1361-648X/acea12.

8. L. Šmejkal, R. González-Hernández, T. Jungwirth et al., *Crystal Time-Reversal Symmetry Breaking and Spontaneous Hall Effect in Collinear Antiferromagnets*, Sci. Adv. **6**, eaaz8809 (2020).

9. R. Chen, Z.-M. Wang, K. Wu et al., *Probing k-Space Alternating Spin Polarization via the Anomalous Hall Effect*, Phys. Rev. Lett. **135**, 096602 (2025); https://doi.org/10.1103/yrs7-m6zy; arXiv:2501.14217.

10. R. D. Gonzalez Betancourt, J. Zubáč, R. Gonzalez-Hernandez et al., *Spontaneous Anomalous Hall Effect Arising From An Unconventional Compensated Magnetic Phase in a Semiconductor*, Phys. Rev. Lett. **130**, 036702 (2023).

11. K. P. Kluczyk, K. Gas, M. J. Grzybowski et al., *Coexistence of Anomalous Hall Effect and Weak Magnetization in a Nominally Collinear Antiferromagnet MnTe*, Phys. Rev. B **110**, 155201 (2024).

12. M. Leiviskä, J. Rial, A. Badura et al., *Anisotropy of the Anomalous Hall Effect in Thin Films of the Altermagnet Candidate* Mn_5Si_3, Phys. Rev. B **109**, 224430 (2024).

13. S. Hayami and H. Kusunose, *Essential Role of the Anisotropic Magnetic Dipole in the Anomalous Hall Effect*, Phys. Rev. B **103**, L180407 (2021).

14. M. Roig, Y. Yu, R. C. Ekman et al., *Quasi-Symmetry Constrained Spin Ferromagnetism in Altermagnets*, Phys. Rev. Lett. **135**, 016703 (2025); arXiv:2412.09338.

15. I. I. Mazin, *Altermagnetism in MnTe: Origin, Predicted Manifestations, and Routes to Detwinning*, Phys. Rev. B **107**, L100418 (2023).

16. D. Kriegner, K. Výborný, K. Olejník et al., *Multiple-Stable Anisotropic Magnetoresistance Memory in Antiferromagnetic MnTe*, Nat. Commun. **7**, 11623 (2016).

17. S. Greenwald, *The Antiferromagnetic Structure Deformations in CoO and MnTe*, Acta Crystallogr. **6**, 396 (1953).

18. T. Komatsubara, M. Murakami, and E. Hirahara, *Magnetic Properties of Manganese Telluride Single Crystals*, J. Phys. Soc. Jpn. **18**, 356 (1963); https://doi.org/10.1143/JPSJ.18.356

19. N. Kunitomi, Y. Hamaguchi, and S. Anzai, *Neutron Diffraction Study on Manganese Telluride*, J. Phys. (Paris) **25**, 568 (1964).

20. M. Podgorny and J. Oleszkiewicz, *Electronic Structure of Antiferromagnetic MnTe*, J. Phys. C **16**, 2547 (1983).

21. E. Przezdziecka, E. Kaminska, E. Dynowska et al., *Preparation and Characterization of Hexagonal MnTe and ZnO Layers*, Phys. Status Solidi C **2**, 1218 (2005).

22. N. N. Orlova, A. A. Avakyants, A. V. Timonina et al., *Crossover from Relativistic to Non-Relativistic Net Magnetization for MnTe Altermagnet Candidate*, JETP Lett. **120**, 360 (2024); https://doi.org/10.1134/S0021364024602926.

23. N. N. Orlova, V. D. Esin, A. V. Timonina et al., *Magnetization Symmetry for the Altermagnetic Candidate MnTe*, Phys. Rev. B **111**, 224414 (2025); https://doi.org/10.1103/br1r-bjzk.

24. M. Hajlaoui, S. W. D'Souza, L. Šmejkal et al., *Temperature Dependence of Relativistic Valence Band Splitting Induced by an Altermagnetic Phase Transition*, Adv. Mater. **36**, 2314076 (2024).

25. N. N. Orlova, V. D. Esin, A. V. Timonina et al., *Magnetocaloric Effect for the Topological Semimetal* $Co_3Sn_2S_2$ *Due to the Antiferromagnetic Coupling of the Bulk and Surface Spin-Polarized Phases*, J. Magn. Magn. Mater. **624**, 172998 (2025); https://doi.org/10.1016/j.jmmm.2025.172998.

26. A. R. Hayyu, S. Baran, and A. Szytuła, *Magnetocaloric Performance of* $RE_5Pd_2In_4$ *(RE = Tb–Tm) Compounds*, Physica B **710**, 417184 (2025); arXiv:2402.17912 (2024).

27. J. Lyubina, *Magnetocaloric Materials for Energy Efficient Cooling*, J. Phys. D: Appl. Phys. **50**, 053002 (2017); https://doi.org/10.1088/1361-6463/50/5/053002.

28. A. A. Avakyants, N. N. Orlova, A. V. Timonina et al., *Surface Spin Polarization in the Magnetic Response of GeTe Rashba Ferroelectric*, JETP Lett. **119**, 625 (2024); https://doi.org/10.1134/S0021364024600605.

29. D. Kriegner, H. Reichlova, J. Grenzer et al., *Magnetic Anisotropy in Antiferromagnetic Hexagonal MnTe*, Phys. Rev. B **96**, 214418 (2017); https://doi.org/10.1103/PhysRevB.96.214418.

30. A. M. Tishin and Y. I. Spichkin, *The Magnetocaloric Effect and its Applications*, CRC Press, Boca Raton (2003); https://doi.org/10.1201/9781420033373.

31. V. Franco, *Determination of the Magnetic Entropy Change from Magnetic Measurements: the Importance of the Measurement Protocol*, Lake Shore Cryotronics, Westerville, Ohio (2015); www.lakeshore.com.

32. G. Hoogeboom, *Spin Transport and Spin Dynamics in Antiferromagnets*, PhD Thesis, University of Groningen, Groningen (2021); https://doi.org/10.33612/diss.157444391.

33. F. Grønvold, N. J. Kveseth, F. Dos Santos Marques et al., *Thermophysical Properties of Manganese Monotelluride from 298 to 700 K. Lattice Constants, Magnetic Susceptibility, and Antiferromagnetic Transition*, J. Chem. Thermodyn. **4**, 795 (1972).

34. M. M. H. Polash, M. Rasoulianboroujeni, and D. Vashaee, *Magnon and Spin Transition Contribution in Heat Capacity of Ferromagnetic Cr-Doped MnTe: Experimental Evidence for a Paramagnetic Spin-Caloritronic Effect*, Appl. Phys. Lett. **117**, 043903 (2020); https://doi.org/10.1063/5.0011887.

35. M. Földeáki, R. Chahine, and T. K. Bose, *Magnetic Measurements: a Powerful Tool in Magnetic Refrigerator Design*, J. Appl. Phys. **77**, 3528 (1995); https://doi.org/10.1063/1.358648.

36. S.-W. Cheong and F.-T. Huang, *Altermagnetism with Non-Collinear Spins*, npj Quantum Mater. **9**, 13 (2024); https://doi.org/10.1038/s41535-024-00626-6.

37. A. Hariki, A. Dal Din, O. J. Amin et al., *X-Ray Magnetic Circular Dichroism in Altermagnetic* α*-MnTe*, Phys. Rev. Lett. **132**, 176701 (2024).